AMSI
AUSTRALIAN MATHEMATICAL SCIENCES INSTITUTE
National Collaboration in the Mathematical Sciences

Waves in Sea Ice

Ewan Short

April 27, 2013

Abstract

The goal of this project is to investigate current methods for modelling the effect of ocean waves on the sea ice cover, and conduct sensitivity analyses on the model developed by Williams, Bennetts, Squire, Dumont and Bertino. (Williams et al. 2013)

1 Introduction

With climate change causing a reduction in the polar ice covers, commercial activity in these regions has increased and there is therefore more demand for high precision predictions regarding the structure of sea ice covers. Although no ice-ocean models currently include wave-ice effects, the notion of doing so goes back almost two decades (Williams et al. 2013, pp.1-4). With recent advances in theory, computational power and measurement accuracy, a working model that deals with these effects is now within reach. The Waves in Ice Model (WIM) is the first attempt at such a model. It has been developed by a number of researchers around the world over the last decade (Williams et al. 2013) and forms the focus of this project.

2 Model Outline

Here we present a rough description of how WIM is structured. First note that sea ice covers can usually be divided up into two portions. These include a region of relatively solid ice we call *pack ice* and a region of *broken ice floes* we call the *marginal ice zone* (MIZ), where broken ice floes are just chunks of broken ice. WIM accepts data on waves in the open ocean, and outputs the length of the MIZ and the floe size distribution (FSD) (see Figure 1).

Postal Address: 111 Barry Street
c/- The University of Melbourne
Victoria 3010 Australia

Email: enquiries@amsi.org.au
Phone: +61 3 8344 1777
Fax: +61 3 9349 4106
Web: www.amsi.org.au

Waves in the model are described by a *spectral density function* $S(\omega, x, t)$, which provides the distribution of angular frequencies ω at each point x in the domain at time t. These functions are useful because their moments provide important wave statistics. We define the n^{th} moment by:

$$m_n = \int_0^\infty \omega^n S(\omega)\, d\omega$$

From which we can obtain the *peak period* T_p and *significant wave height* H_s by:

$$T_p = 2\pi \frac{m_0}{m_1},\ H_s = 4\sqrt{m_0}$$

These quantities represent the average period of the waves in the spectrum, and the dominant wave height respectively. Note that there is no directional parameter in S because WIM is one dimensional, thus we disregard the waves not travelling directly along the modelled cross section. The input wave data is provided in the form of a Bretshneider spectrum:

$$S(\omega, 0, t) = S_B(\omega, T_p, H_s) = \frac{1.25 H_s^2 T^5}{8\pi T_p^4} e^{-1.25(T/T_p)^4}$$

where $T = \frac{2\pi}{\omega}$.

The wave spectrum is moved through the ice by solving the wave energy balance equation:

$$\frac{1}{c_g} D_t S = \frac{1}{c_g}\left(\frac{\partial S}{\partial t} + c_g \frac{\partial S}{\partial x}\right) = -\hat{\alpha} S$$

where $c_g(\omega)$ is the *group velocity*, $\hat{\alpha}$ is the *attenuation coefficient* and D_t is the material derivative. The group velocity can be thought of as the speed the waves centred around a particular frequency are travelling. The attenuation coefficient gives the rate at which energy is lost as the waves move through the ice, and is mainly determined by wave scattering at the edges of individual floes. This means that it depends on the extent of ice breakage, so we need to check for breakage as the spectrum moves. This is implemented in WIM by discretising the ω, x and t domains of S and checking for breakage only at the end of each time step. We can then show using Lagrangian coordinates that the advection of S, which is the distance the spectrum travels, and the attenuation of S can be calculated separately between breaking events. To calculate the advection we simply solve the wave energy balance equation without resistance:

$$D_t S = \frac{\partial S}{\partial t} + c_g \frac{\partial S}{\partial x} = 0$$

numerically at each time step, and store the result in the intermediate spectrum $\hat{S}$. To calculate the attenuation we derive the approximation:

$$S^n_{j,r} \approx \hat{S}^n_{j,r} \exp(-\hat{\alpha}^n_{j,r} c_g \Delta t)$$

from $\frac{1}{c_g} D_t S = -\hat{\alpha} S$ (Appendix A.1). The relation governing $\hat{\alpha}$ is complex, so a finite range of values is pre-calculated, then interpolated.

To check for ice breakage, we use S to calculate $\mathbb{P}_\epsilon$, the probability the ice will break. We choose a critical probability $\mathbb{P}_c$, and if $\mathbb{P}_\epsilon > \mathbb{P}_c$ we reduce the maximum floe size at the current x grid point to $\frac{\lambda}{2}$ where λ is the average wavelength of the spectrum.

WIM is implemented in MatLab. At each time step we iterate through the time domain, and at each time step,

1. Advect S,
2. Iterate through our spatial domain and for each x grid point,
   (a) Calculate the attenuation of S,
   (b) Check for ice breakage.

3 Investigations

I began my project by attempting to understand in detail how the model works. My supervisor was unfamiliar with the numerical scheme used in the advection step and asked me to investigate. I then became curious about the approximation used in the attenuation step and attempted to derive it myself.

3.1 Advection Equation

During the advection step we assume there is no resistance to the waves, so the wave energy balance equation reduces to $D_t S = 0$. The model is able to use a variety of numerical methods to solve this equation, although it's authors recommend the default choice of the Lax Wendrof scheme with Superbee flux limiting. The Lax Wendrof scheme is a finite difference method (FDM) with second order accuracy in both space and time. It provides numerical solutions to equations of the form:

$$\frac{\partial f(x,t)}{dt} = \frac{\partial g(f(x,t))}{\partial x}$$

where $f(x,0)$ is given. It acts in two steps, first calculating $f_{i\pm1/2}^{n+1/2}$ from:

$$\frac{f_{i\pm1/2}^{n+1/2} - \frac{f_i^n + f_{i\pm1}^n}{2}}{(1/2)\Delta t} = \frac{g_{i+1}^n - g_i^n}{\Delta x}$$

and then f_i^{n+1} from:

$$\frac{f_i^{n+1} - f_i^n}{\Delta t} = \frac{g_{i+1/2}^{n+1/2} - g_{i-1/2}^{n+1/2}}{\Delta x}$$

When solving for f, we define the flux at i, n to be:

$$F_i^n = g(f_i^n)$$

Flux limiting is used in high resolution schemes to reduce excessive oscillations around sharp changes in slope. We first approximate the flux by some scheme:

$$F_i^n \approx G_i^n + h_i^n$$

where G_i^n is a low order approximation and h_i^n is a higher order term. We then define the variable r_i^n by:

$$r_i^n = \frac{f_i^n - f_{i-1}^n}{f_{i+1}^n - f_i^n}$$

which measures the rate at which f is changing. Finally we can introduce the flux limiter function $\phi(r_i)$ and write:

$$F_i^n = G_i^n + \phi(r_i) h_i^n$$

The only requirement on ϕ is that it be non negative, but the idea is that for extreme values of r only the lower order approximation is used, but for r close to 1 the higher order term is included. The authors recommend that the Superbee flux limiter $\phi(r) = \max[0, \min(2r, 1), \min(r, 2)]$ be used in the WIM.

Rearranging the wave energy balance equation, we have:

$$D_t S = 0 \Rightarrow \frac{\partial S}{\partial t} + c_g \frac{\partial S}{\partial x} = 0 \Rightarrow \frac{\partial S}{\partial t} = -c_g \frac{\partial S}{\partial x}$$

where c_g is the group velocity. This is of the form to which we can apply the Lax-Wendrof scheme, taking $S = f$ and $g(f) = -c_g S$. From the first step of the scheme we can calculate:

$$F_{i\pm1/2}^{n+1/2} = -c_g S_{i\pm1/2}^{n+1/2} = -c_g S_i^n - \frac{c_g}{2}\left(1 - c_g \frac{\Delta t}{\Delta x}\right)\left(S_{i+1}^n - S_i^n\right)$$

where $-c_g S_i^n$ is thought of as a low order approximation to $-c_g S_{i\pm1/2}^{n+1/2}$ and

$$-\frac{1}{2}\left(1 - c_g\frac{\Delta t}{\Delta x}\right)\left(s_{i+1}^n - S_i^n\right)$$

is thought of as a higher order term. We thus apply the Superbee flux limiter function to this higher order term and obtain:

$$-c_g S_{i\pm1/2}^{n+1/2} = -c_g S_i^n - \frac{c_g}{2}\left(1 - c_g\frac{\Delta t}{\Delta x}\right)\left(S_{i+1}^n - S_i^n\right)\phi(r_{i\pm1})$$

We can then calculate S_i^{n+1} from the second step of the Lax-Wendroff scheme.

3.2 Attenuation Equation

After advection, we calculate the attenuation due to ice resistance. When we include ice resistance in the wave energy balance equation we obtain:

$$\frac{1}{c_g}D_t S(\omega, x.t) = -\hat{\alpha}(\omega, c, h, \langle D\rangle)S(\omega, x, t)$$

where $\hat{\alpha}$ depends explicitly on wave frequency ω, ice concentration c, height h, and average floe size $\langle D\rangle$, so implicitly on just ω, x and t. This equation can be expressed in Lagrangian coordinates as $\frac{d}{dx}S = -\hat{\alpha}S$ where $\frac{dx}{dt} = c_g$ (Appendix A.1). By integrating and approximating, we obtain:

$$S_{j,r}^n \approx \hat{S}_{j,r}^n \exp(-\hat{\alpha}_{j,r}^n c_g \Delta t)$$

Alternatively, we can derive (Appendix A.1),

$$S_{j,r}^n \approx \hat{S}_{j,r}^n \exp\left(\frac{1}{2}\left[(C-2)\hat{\alpha}_{j,r}^n - C\hat{\alpha}_{j-1,r}^n\right]c_g\Delta t\right)$$

where $C = c_g\frac{\Delta t}{\Delta x}$ is the Courant number, which gives the proportion of one grid cell the spectrum travels through in on time step.

Currently the model is coded so that users have a choice as to whether they use ice data from the current or previous x grid step when calculating attenuation. This essentially means users can choose whether or not to use ice that has already been broken up by the spectrum in the current time step.

When using the former attenuation formula with ice data from the previous spatial grid step, there is no sensitivity to Courant number C. Using the second formula introduces sensitivity as the amount of broken ice the wave travels through now depends on C. However, when using ice data from the current grid step the original formula is quite sensitive to C, but this is reduced when using the new formula. This is because the new formula essentially weights the contribution of previous and current grid step ice data to the total attenuation by the speed the spectrum is travelling. However this is not overly important, as when $C = 1$ the results in each case are almost identical and we can usually choose our x and t steps to give $C = 1$. However, when we allow different frequencies in the spectrum to travel at different speeds or extend the model to two dimensions, it may become important.

4 Sensitivity Tests

I then conducted a series of sensitivity tests, reproducing the tests in the Williams et al. paper (Williams et al. 2013) and then devising my own. The two most interesting of these were sensitivity to different incident wave spectra and sensitivity to different values for the Young's modulus of the ice.

4.1 Spectra

The input open ocean wave data is parametrized with the Bretshneider spectrum:

$$S(\omega, 0, t) = S_B(\omega, T_p, H_s) = \frac{1.25 H_s^2 T^5}{8\pi T_p^4} e^{-1.25(T/T_p)^4}$$

where T is wave period, T_p is the peak or average wave period, and H_s is the significant wave height. Note that $T = \frac{2\pi}{\omega}$, where ω is frequency. The default values used for testing were $T_p = 9.5$, $H_s = 3$. The integral over ω of any wave spectrum S is called the *zeroth moment*. It is denoted m_0, and must satisfy $m_0 = \frac{1}{16} H_s^2$.

Broadly speaking, there are two ways ocean waves are formed in the open ocean. *Fetch waves* are generated by winds acting over long distances with typical periods of $13 - 14$ seconds, whereas *swell waves* are formed by gravity and typically have shorter periods. We therefore should test how the model behaves to incident wave spectra with two peaks, rather than one. To do this we need to ensure all the spectra possess the same total energy. Total energy is proportional to H_s^2, and we can obtain new spectra with a given value of H_s^2 by superimposing spectra with significant wave height H_1 and H_2 such that $H_1^2 + H_2^2 = H_s^2$ (Appendix A.2). In Figure 2 we plot how the model

responds to a selection of spectrums obtained by superimposing two Bretschneider spectrums of peak period 6 and 13 seconds respectively, with varying fractions of the total wave energy coming from each. For example, the green line corresponds to a spectrum with 75 percent of its energy associated with a peak period of 6 seconds, and 25 percent associated with a peak period of 13 seconds.

Immediately we see that when high frequencies are dominant, the maximum flow sizes in the MIZ are small, as when the ice breaks the maximum floe size is reduced to half the average wavelength. Also, the length of the MIZ is smaller, as high frequencies cannot penetrate very far into the ice cover.

To test sensitivity to just the shape of different spectrums, we must ensure they have the same average periods. To do this we define the *normal spectrum* by:

$$S_N(\omega) = \frac{H_s^2}{16\sigma\sqrt{2\pi}} e^{-\frac{1}{2}\left(\frac{\omega-\omega_p}{\sigma}\right)^2}$$

We can then superimpose two normal spectrums with significant wave height $\sqrt{4.5}$ metres and peak periods of approximately 6.314 and 13 seconds respectively, and compare the results with a normal spectrum of significant wave height 8.5 metres and a peak period of 9 seconds. We can show (Appendix A.2) that the sum of the first two spectrums also has a significant wave height of 3 metres and a peak period of 8.5 seconds. The output of the model is plotted in Figure 3.

We can see from this that the presence of low frequency waves changes the length of the MIZ by at least 30km. From this we can conclude that the model is sensitive to spectrum shape, in particular to the spread of the spectrum and the presence of low frequency waves.

4.2 Young's Modulus

Currently the model assumes a fixed value for the Young's Modulus of the sea ice, $Y = 5$ G Pa, but this is problematic as sea ice is an inhomogenous material and Y will vary throughout. We therefore wish to test how sensitive the model is to variations in Y. To do this we simply include an extra dimension to our look-up table for the attenuation coefficient, and use a simpler interpolation method.

In Figure 4 we plot the model output for different values of Y. From the plot, it appears that only the length of the MIZ is affected by varying Y. However, the maximum floe sizes at the points where the curves appear to lie on top of one another actually differ after the tenth decimal place. This difference can be exacerbated by changing the peak period of the incident spectrums.

These results are perhaps unphysical, and point to a need to investigate the behaviour of the numerics used when testing different values of Y.

5 Conclusions

This project has provided me with valuable insight into the challenges of modelling physical systems. Making progress requires not only knowledge of the physical system and its deterministic mathematical formulation, but skills with numerical methods, probability and computer science in order to implement the model on a computer. I learned a number of important lessons throughout this project as to the importance of numerical methods in producing accurate models, and how the way in which a mathematical model is translated into a computer algorithm can deeply affect the results produced. The project has inspired me to continue studying this field for my honours project, with the goal of extending the model to two spatial dimensions.

I have thoroughly enjoyed this project and attending the CSIRO Big Day In. I would like to thank AMSI and CSIRO for the opportunity and my supervisor Dr. Luke Bennetts for his encouragement and support.

A Calculations

A.1 Attenuation Coefficient

In one spatial dimension $D_t = \frac{d}{dt}$. If we fix ω and consider the spectrum in Lagrangian coordinates, we take x to be a function $x(x_0, t)$, which gives the position at time t of the point of the wave spectrum initially at x_0. If we fix x_0 and vary x, then t becomes a function $t(x, x_0)$, which gives the time the point initially at x_0 arrives at x. We can then calculate $\frac{dx}{dt} = c_g$, so $\frac{dt}{dx} = \frac{1}{c_g}$ by the inverse function theorem, and thus $\frac{1}{c_g} D_t S = \frac{dt}{dx}\frac{d}{dt} S = \frac{d}{dx} S$ by the chain rule. We can therefore rewrite $\frac{1}{c_g} D_t S = -\hat{\alpha} S$ as:

$$\frac{d}{dx} S = -\hat{\alpha} S$$

Postal Address: 111 Barry Street
c/- The University of Melbourne
Victoria 3010 Australia

Email: enquiries@amsi.org.au
Phone: +61 3 8344 1777
Fax: +61 3 9349 4106
Web: www.amsi.org.au

Solving this equation we obtain:

$$\begin{aligned}
&\frac{d}{dx}S(x,t(x,x_0)) = -\hat{\alpha}(x,t(x,x_0))S(x,t(x,x_0)) \\
\Rightarrow &\frac{dS}{dx}\frac{1}{S} = -\hat{\alpha} \\
\Rightarrow &\int_a^x \frac{dS}{dx}\frac{1}{S}\,dx = \int_a^x -\hat{\alpha}\,dx \qquad \text{(for constant } a < x\text{)} \\
\Rightarrow &\log(S(x,t(x,x_0))) - \log(S(a,t(a,x_0))) = \int_a^x -\hat{\alpha}\,dx \\
\Rightarrow &S(x,t(x,x_0)) = S(a,t(a,x_0))e^{\int_a^x -\hat{\alpha}\,dx}
\end{aligned}$$

If the distance between a and x is small, we can approximate $\int_a^x -\hat{\alpha}\,dx$ by $\hat{\alpha}(x,t(x,x_0))\cdot(x-a)$ and write:

$$S(x,t(x,x_0)) \approx S(a,t(a,x_0))e^{-\hat{\alpha}(x,t(x,x_0))\cdot(x-a)}$$

Let $\hat{S}(x,t(x,x_0))$ denote the spectrum after advection but before attenuation. If we set $x = a + c_g\Delta t$, where Δt is the time step used in our numerical scheme, we have:

$$S(a,t(a,x_0)) = S(a,t(x,x_0) - \Delta t) = \hat{S}(x,t(x,x_0))$$

and so

$$S(x,t(x,x_0)) \approx \hat{S}(x,t(x,x_0))e^{-\hat{\alpha}(x,t(x,x_0))\cdot c_g\Delta t}$$

If we take x to be a spatial grid point in our numerical scheme, we can discretise to obtain,

$$S^n_{j,r} \approx \hat{S}^n_{j,r}\exp(-\hat{\alpha}^n_{j,r}c_g\Delta t)$$

Instead of approximating $\int_a^x -\hat{\alpha}\,dx$ by $\hat{\alpha}(x,t(x,x_0))\cdot(x-a)$, we could also use the mid point rule,

$$\int_a^x -\hat{\alpha}\,dx \approx \frac{-\hat{\alpha}(x,t(x,x_0)) - \hat{\alpha}(a,t(a,x_0))}{2}\cdot(x-a)$$

However, if we set $x = a+c_g\Delta t$ as before, then $t(a,x_0) = t(x,x_0)-\Delta t$ and $a = x-c_g\Delta$ will only lie on a spatial grid point if $c_g\Delta t = \Delta x$, that is, if the courant number $C = \frac{c_g\Delta t}{\Delta x} = 1$. However if $C < 1$, we can write:

$$\begin{aligned}
-\hat{\alpha}(a,t(a,x_0)) &= -\hat{\alpha}(x - c_g\Delta t, t(x,x_0) - \Delta t) \\
&\approx -(1-C)\hat{\alpha}(x,t(x,x_0)-\Delta t) - C\hat{\alpha}(x-\Delta x, t(x,x_0)-\Delta t)
\end{aligned}$$

Postal Address: 111 Barry Street
c/- The University of Melbourne
Victoria 3010 Australia

Email: enquiries@amsi.org.au
Phone: +61 3 8344 1777
Fax: +61 3 9349 4106
Web: www.amsi.org.au

We can then sub this into the midpoint rule and discretise to obtain:

$$S_{j,r}^n \approx \hat{S}_{j,r}^n \exp\left(\frac{1}{2}\left[-\hat{\alpha}_{j,r}^n - (1-C)\hat{\alpha}_{j,r}^{n-1} - C\hat{\alpha}_{j-1,r}^{n-1}\right] c_g \Delta t\right)$$

In our numerical scheme we attenuate before we test for ice breakage, so we can replace $-\hat{\alpha}_{j,r}^n$ with $-\hat{\alpha}_{j,r}^{n-1}$, and the above reduces to:

$$S_{j,r}^n \approx \hat{S}_{j,r}^n \exp\left(\frac{1}{2}\left[(C-2)\hat{\alpha}_{j,r}^n - C\hat{\alpha}_{j-1,r}^n\right] c_g \Delta t\right)$$

A.2 Wave Spectrum Energy and Peak Period

If $S = S_1 + S_2$ for spectrums S_1, S_2 with significant wave heights H_1, H_2 respectively, we have:

$$\begin{aligned}\frac{1}{16}H_s^2 &= \int_0^\infty S \; d\omega = \int_0^\infty S_1 + S_2 \; d\omega \\ &= \int_0^\infty S_1 \; d\omega + \int_0^\infty S_2 \; d\omega = \frac{1}{16}H_1^2 + \frac{1}{16}H_2^2\end{aligned}$$

The total energy of the spectrum S is proportion to H_s^2, so we can obtain new spectrums with a given value of H_s^2 by superimposing spectrums with significant wave height H_1 and H_2 such that $H_1^2 + H_2^2 = H_s^2$.

To test sensitivity to the spectrums overall shape, such as the number of peaks it has, we should also make sure the average period is the same between spectrums. The peak period is given by (Formsys 2013)

$$T_p = 2\pi\frac{m_0}{m_1}$$

For simplicity we define a normally distributed wave spectrum:

$$S_N(\omega) = \frac{H_s^2}{16\sigma\sqrt{2\pi}} e^{-\frac{1}{2}\left(\frac{\omega-\omega_p}{\sigma}\right)^2}$$

where $\omega_p = \frac{2\pi}{T_p}$. Note that the first moment of S_N is just $\frac{H_s^2\omega_p}{16}$. Thus if we define $S = S_1 + S_2$ as before, where each spectrum is normally distributed, and S, S_1, S_2 have peak periods T_p, T_1, T_2 respectively, the equation $T_p = 2\pi\frac{m_0}{m_1}$ allows us to derive the equation:

$$T_1 = \frac{H_1^2 T_2 T_p}{T_2 H_s^2 - T_p H_2^2}$$

This allows us to choose T_p and T_2, and combined with the expression $H_s^2 = H_1^2 + H_2^2$ determine T_1 so that $S_1 + S_2$ has the peak period T_p and the same total energy as the single peak spectrum centred at T_p with significant wave height H_s.

A.3 Figures

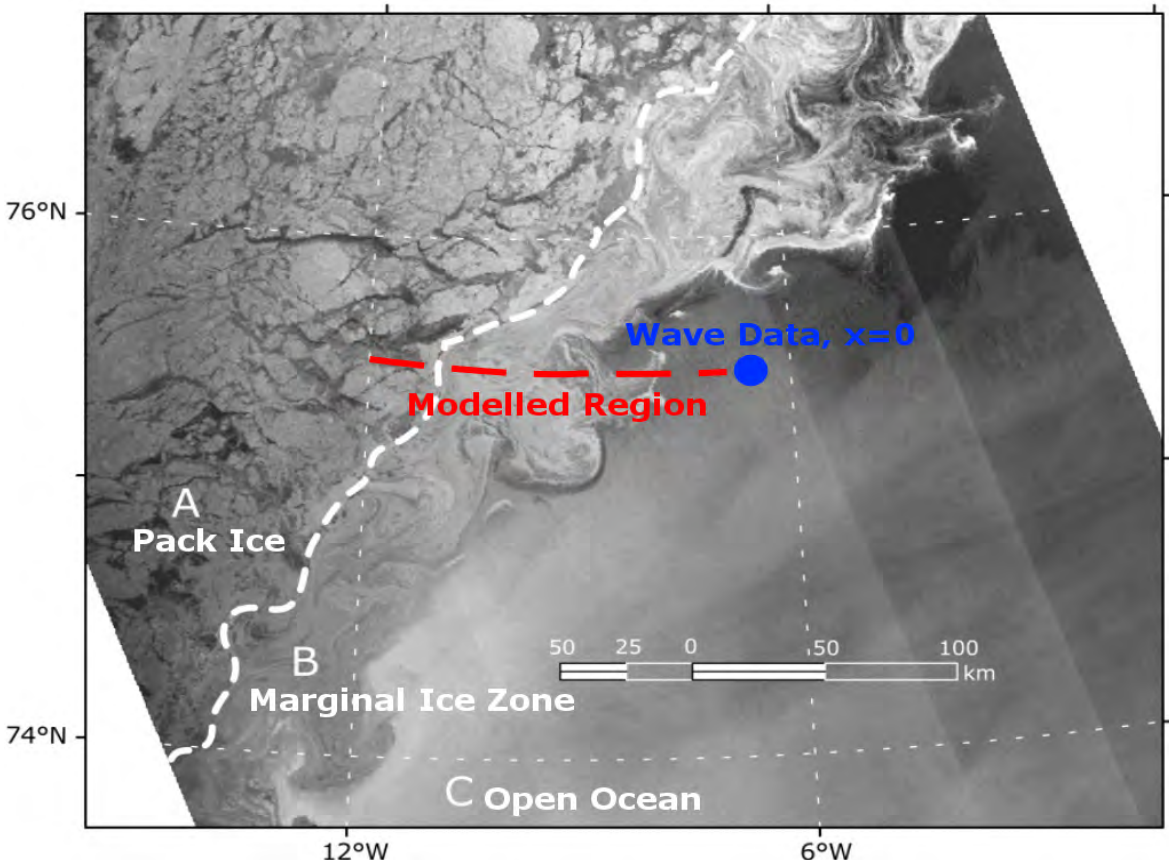

Figure 1: Example modelled region of the MIZ.

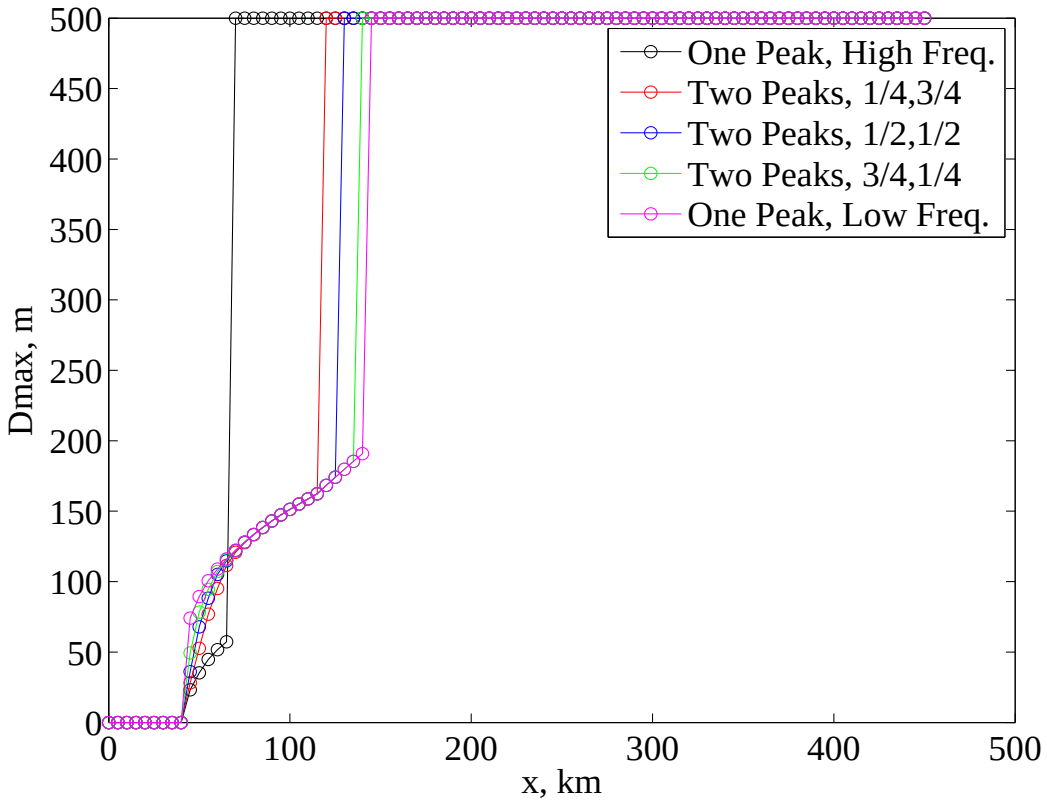

Figure 2: Sensitivity to different superimposed Bretshneider spectrums.

References

Formsys (2013), 'Wave spectra'.
`http://www.formsys.com/extras/FDS/webhelp/seakeeper/wave_spectra1.htm`

Williams, T. D., Bennetts, L. G., Squire, V. A., Dumont, D. & Bertino, L. (2013), 'Wave-ice interactions in the marginal ice zone. part 1: Theoretical foundations', *Ocean Modelling (Submitted)* pp. 1–43.

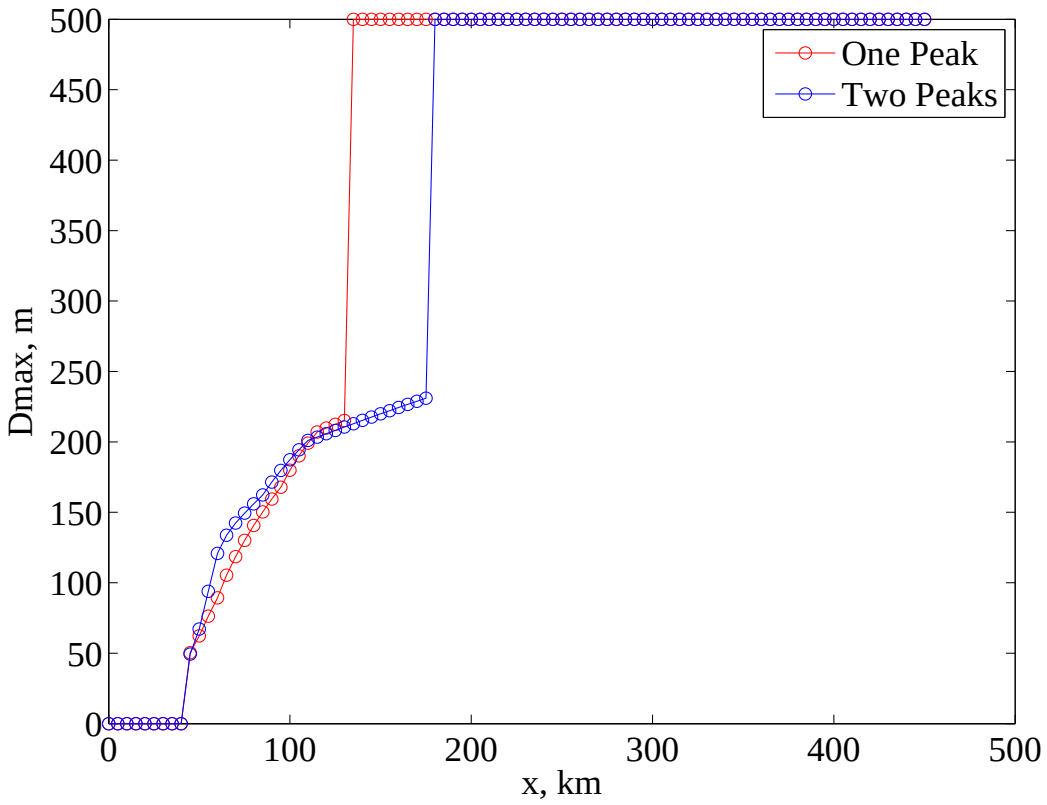

Figure 3: A plot of model sensitivity to incident spectrum shape.

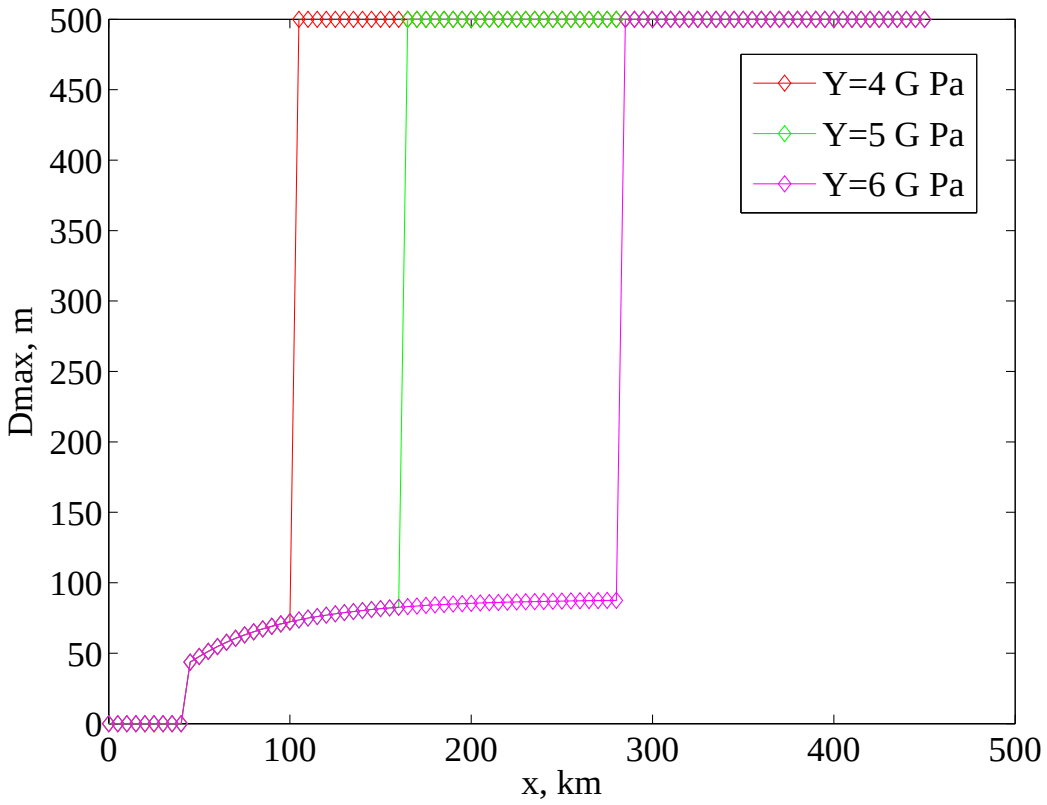

Figure 4: A plot of model sensitivity to Young's Modulus.